



Published in final edited form as:

J Cell Biochem. 2017 November ; 118(11): 3627–3634. doi:10.1002/jcb.26220.

Development of a Cell-Based Gene Therapy Approach to Selectively Turn Off Bone Formation

Pedro Alvarez-Urena¹, Banghe Zhu^{2,3}, Gabrielle Henslee¹, Corinne Sonnet¹, Eleanor Davis¹, Eva Sevick-Muraca², Alan Davis^{1,3,4}, and Elizabeth Olmsted-Davis^{1,3,4,*}

¹Center for Cell and Gene Therapy, Baylor College of Medicine, Texas Children's Hospital and Houston Methodist Hospital, Houston, Texas

²Center for Molecular Imaging, University of Texas Health Sciences Center, Houston, Texas

³Department of Pediatrics—Section Hematology/Oncology, Baylor College of Medicine, Houston, Texas

⁴Department of Orthopedic Surgery, Baylor College of Medicine, Houston, Texas

Abstract

Cell and gene therapy approaches are safer when they possess a system that enables the therapy to be rapidly halted. Human mesenchymal stem cells were transduced with an adenoviral vector containing the cDNA for bone morphogenetic protein 2 (AdBMP2) to induce bone formation. To make this method safer, a system to quickly kill these virally transduced cells was designed and evaluated. Cells were encapsulated inside poly(ethylene glycol) diacrylate (PEG-Da) hydrogels that are able to shield the cells from immunological destruction. The system involves an inducible caspase-9 (iCasp9) activated using a specific chemical inducer of dimerization (CID). Delivering AdBMP2-transduced human mesenchymal stem cells encapsulated in PEG-Da hydrogel promoted ectopic ossification *in vivo*, and the iCasp9 system allowed direct control of the timing of apoptosis of the injected cells. The iCasp9-CID system enhances the safety of delivering AdBMP2-transduced cells, making it a more compelling therapeutic for bone repair and spine fusion.

Keywords

BONE FORMATION; BIOMATERIAL; DELIVERY SYSTEM; CELL THERAPY; INDUCIBLE SUICIDE GENE; *IN VIVO*

Since the discovery of the bone morphogenetic proteins (BMPs) in bone matrix, researchers have been attempting to harness their potential for inducing bone formation [Lo et al., 2012]. Currently, recombinant BMP protein, specifically rhBMP2, has been used to augment bone formation in a variety of settings [Govender et al., 2002]. However, the short half-life of the protein and the large number of binding proteins/inhibitors meant that the protein had to be

*Correspondence to: Elizabeth Olmsted-Davis, PhD, Associate Professor of Pediatrics and Orthopaedic Surgery, Center for Cell and Gene Therapy, Baylor College of Medicine, One Baylor Plaza, N1010 Houston, TX 77030. edavis@bcm.edu.

Conflicts of interest: The authors do not have any conflicts of interests to disclose.

introduced through a carrier [Levy et al., 1986; Boerckel et al., 2011]. Currently, one of the only carriers used clinically is a collagen sponge, which can lead to a robust inflammatory reaction [Gugala et al., 2007; Huang et al., 2017]. Alternatively, it is capable of reducing the release of the protein and providing a longer window of efficacy [Acton, 2012; Huang et al., 2017]. Although other biomaterials are being explored as carriers for BMPs the only carrier currently approved for rhBMP2 is a bovine collagen carrier. Further troubling is that induction of bone formation through delivery of rhBMP2 requires high levels of protein and can result in variable response. These high doses of protein have resulted in complications in patients where they have raised antibodies against the protein [Salisbury et al., 2011], or off target effects on the nervous system [Dmitriev et al., 2010, 2011; Carragee et al., 2011] leading the FDA to issue a warning, and resulting in a significant reduction in its clinical use. Currently, the question of how to harness the potential of BMPs has become a major endeavor of bone researchers, resulting in a number of different carriers and delivery methods, including nanoparticles, in development [Boerckel et al., 2011].

To overcome these problems, many have attempted to implement gene therapy strategies that would provide consistent release of an eukaryotically produced protein over a longer period of time. These strategies involve using viral and nonviral methods to transduce tissues either at the target site or through delivery of cells expressing the protein [Partridge and Oreffo, 2004]. However, these approaches have raised concerns, both in poor transduction efficiencies [Stiehler et al., 2006], potential off target effects, or rapid clearance by the immune system [VandenDriessche and Chuah, 2015]. To avoid this, two different strategies have been employed. The first is to incorporate the BMP2 transgene into the chromosome of mesenchymal stem cells that can be delivered nonautologously [Engstrand et al., 2000] and that can survive at the target site to produce bone. With incorporation of the transgene into cells, no virus would be needed, and issues of immunity could be minimized. Alternatively, integration of the transgene into the chromosome raises concerns that this might potentially disrupt other genes that could lead to adverse events or cancer [Sadelain, 2004]. A second strategy is to use a non-integrating system that would allow the cells to make the transgene as an episome, and therefore, avoid the risk of gene disruption [Olmsted-Davis et al., 2002]. With this strategy, the cells could then be encompassed in hydrogel biomaterials that would allow the cells to survive long term, but alleviate activation of adaptive immune responses and cellular clearance [Olabisi et al., 2010]. A final concern is that when the cells are released during degradation of the biomaterial, they could potentially circulate leading to unwanted bone formation at off-target sites.

To circumvent these problems associated with the use of genetically modified cells, researchers have developed a safety-switch that allows selective killing of the genetically modified cells, which has been evaluated in humans [Di Stasi et al., 2011; Zhou et al., 2015]. The switch is based on caspase 9 and its ability to dimerize activating a cascade of events that results in apoptosis of the engineered cells. In this system, caspase 9 has been engineered to be inducible (icasp9) through delivery of a small molecule. Thus, this gene can be integrated into the genome of the delivery cell, which can be killed within 30 min by delivery of the chemical inducer of dimerization (CID) [Di Stasi et al., 2011].

The ability of the CID to effectively regulate BMP2 expression and end bone formation has not been tested. In this study, the ability to terminate BMP2 at various stages during the process of bone formation was examined. Bone morphogenetic protein 2 (BMP2) was introduced into cells using a replication-defective adenovirus that contains the transgene. The cells were then encapsulated in a poly (ethylene glycol) diacrylate (PEG-Da) hydrogel and injected into the soft tissue of the hamstrings of mice [Olmsted-Davis et al., 2002; Olabisi et al., 2010]. PEG-Da possesses a hydrophilic polymeric network, which increases their biocompatibility and makes them a widely used biomaterial for tissue engineering [Olabisi et al., 2010]. The goal of this study is to test the safety switch introduced into the encapsulated cells and determine whether it can regulate the new bone formation. The results confirm that the safety switch is easily regulated in vivo through systemic injection of the CID, even in cells encapsulated in PEG-Da hydrogel. Surprisingly, kinetic studies where the reaction was terminated early, show an essential role for the BMP2 throughout the entire period of bone formation, suggesting that BMP2 does not function as a trigger, but rather must remain present at the site above threshold levels in order for any bone to form. Additionally, the studies demonstrated the ability to terminate the cells after bone formation without deleterious effects on the newly formed bone. Therefore, these studies support the idea that PEG-Da encapsulation for delivering AdBMP2-transduced hMSC-iCasp9 cells could be a compelling methodology for both bone repair and spine fusion.

MATERIALS AND METHODS

CELL CULTURE OF MESENCHYMAL STROMAL CELLS

Human mesenchymal stromal cells (hMSCs) previously transduced with the inducible caspase 9 (iCasp9) suicide system were obtained from Carlos Ramos at the Center for Cell and Gene Therapy (Baylor College of Medicine, Houston, TX) and were propagated as previously described [Straathof et al., 2005]. The hMSC-iCasp9 cells were propagated in a humidified incubator at 35°C/5% CO₂ in Alpha-MEM medium (Invitrogen Life Technologies, Waltham, MA) supplemented with 16.5% fetal bovine serum, 100,000 U/L penicillin, 100 mg/L streptomycin, and 0.25 mg/L amphotericin B (Invitrogen Life Technologies, Waltham, MA).

ADENOVIRUSES AND CELL TRANSDUCTION

A replication defective first generation human type 5 adenovirus (Ad5) with deleted regions E1 and E3 was constructed to contain the cDNA for human BMP2 and far-red fluorescent protein (iRFP) in the E1 region of the viral genome, as previously described [Olmsted-Davis et al., 2002]. The viruses were confirmed to be negative for replication competent adenovirus, and virus particle (vp) to plaque-forming unit (pfu) ratios were 1:21 and 1:36, respectively. hMSC-iCasp9 cells were transduced with Ad5BMP2 at a concentration of 3,000 vp/cell and Ad5iRFP at a concentration of 2,000 vp/cell with GeneJammer (Agilent Technologies, Santa Clara, CA) [Fouletier-Dilling et al., 2005]. Transduction efficiency was greater than 90%.

IN VIVO STUDIES

All animal studies were performed with Baylor College of Medicine Institutional Animal Care and Use Committee approval in accordance with OLAW guidelines. Animals, male and female, were randomly selected based on age and health and placed in experimental groups. Each animal was given an experimental number that is linked only to its group in the medical record. Therefore, experimenters involved in data collection and analysis were blinded, and the animal numbers only linked back to groups for the final data analysis. Group sizes were based on historical power analysis data; however, all power analysis was repeated after data collection to confirm group sizes were adequate.

BMP-dependent bone formation and cellular response to CID was assessed by delivering 5×10^6 AdBMP2-AdiRFP co-transduced hMSCs-iCasp9 cells either microencapsulated in PEGDA hydrogel (150 micron average diameter [Olabisi et al., 2010]), or directly injected to NOD/SCID mice (Charles River Laboratories) and then following the cells through far-red infrared imaging. Bone formation was assessed at 2 weeks using microCT. Mice received an intraperitoneal injection (IP) of 50 μ g of CID AP1903 (AP1903: 5 mg/ml stock, Bellicum Pharmaceuticals, Houston, TX) or vehicle (media) at times indicated in the text.

MICROENCAPSULATION

PEG-Da was synthesized by reacting 10 kDa PEG with a twofold molar excess of acryloyl chloride as previously described [Olabisi et al., 2010; Hsu et al., 2011]. Hydrogel precursor solutions were prepared by combining 0.1 g/ml 10 kDa PEG-Da (10% w/v) with 1.5% (v/v) triethanolamine/HEPES-buffered saline (pH 7.4), 37 mM 1-vinyl-2-pyrrolidinone, 0.1 nM eosin Y, 0.1% pluronic F68, and transduced hMSC-iCasp9 cells for a final concentration of 5×10^6 cells/ml. A hydrophobic photoinitiator solution (2,2-dimethoxy-2-phenylacetophenone in 1-vinyl-2-pyrrolidinone; 300 mg/ml, Sigma-Aldrich, St. Louis, MO) was combined in mineral oil (3 ml/ml, embryo tested, sterile filtered; Sigma-Aldrich). The microspheres were formed after adding the hydrogel precursor solution into the mineral oil and emulsifying by vortex for 2 s, while exposing to white light for an additional 20 s. Microspheres were isolated through centrifugation at 330g.

CID VIABILITY ASSAYS

To test the response of the iCasp9 in the transduced encapsulated cells, 50 nM of CID AP1903 (AP1903: 5 mg/ml stock, Bellicum Pharmaceuticals) or vehicle (media) was added to the microspheres, and 24 h later cellular viability was tested using a LIVE/DEAD cell viability stain (ThermoFisher Sci, Waltham, MA).

ALKALINE PHOSPHATASE ASSAY

W20-17 cells were assayed for alkaline phosphatase activity by a chemiluminescent procedure [Olmsted et al., 2001]. Briefly, culture supernatant from AdBMP2 transduced hMSCs-iCasp-9 cells cultured in CID or vehicle as indicated in text, was added to the W20-17 cells, and alkaline phosphatase activity was measured 3 days later. The sample mean and standard deviations were calculated and compared using a student *T*-test using a 95% confidence interval ($P < 0.05$).

LIVE ANIMAL OPTICAL FLUORESCENT IMAGING

Far-red fluorescence imaging was performed on the mice for days as specified using an intensified CCD (ICCD) camera-based imaging system [Azhdarinia et al., 2011]. Briefly, a laser diode operating at 690 nm wavelength (HPD 1305-9mm-69005 model, Intense, NJ, USA) was used to excite the iRFP protein, and the emitted signals were collected through 720 nm band pass filter (720FS10, optical density >4, FIRXray, Andover, Salem, NH) and recorded by the ICCD camera. The illumination power on the mice was 1.0 mW/cm², the integration times of ICCD camera were 200 ms, and the gain of intensifier was set to a constant value. Image analysis was performed using ImageJ (a public software developed by the National Institute of Health). Fluorescence intensity was measured over a region of interest for each site of the animal injected with cells.

MICRO-CT IMAGING

Microcomputed tomography (micro-CT) was performed 10 days after delivery of the cells. After euthanasia, the hind limbs were examined at a 15 mm resolution (eXplore Locus SP; GE Healthcare, London, ON, Canada). A hydroxyapatite phantom was scanned alongside each specimen and was used to convert the scan data from arbitrary units to units of equivalent bone density. The three-dimensional region of interest was defined for each animal to separate ectopic bone from the normal skeletal structures. The threshold for tissue within the region of interest was set to exclude any tissue with a density less than 100 mg/cc, and the volume of tissue was calculated as a total amount of mineralized tissue.

HISTOLOGY

Tissues, after microCT analysis, were decalcified, formalin fixed, and subjected to paraffin embedding. Serial sections (4 microns) were generated throughout the entire mouse hind-limb, and every 5th slide was subject to hematoxylin and eosin staining.

STATISTICAL ANALYSIS

All data were reported as mean \pm standard deviation. Statistical analysis included a one-way analysis of variance (ANOVA) with Tukey-Kramer's post hoc test at a significance level of P 0.05.

RESULTS

IN VITRO VALIDATION OF iCasp9 SAFETY SWITCH

To confirm that the chemical inducer of dimerization (CID) was inducing apoptosis in the human mesenchymal stem cells (hMSCs) that have a stably integrated copy of the inducible caspase 9 (icasp), the cells were exposed to either CID or vehicle and cell death measured 1 day later (Fig. 1). The results suggest that the CID had an extremely potent cytotoxic effect with 99 percent loss in cell viability as compared to the vehicle-treated group. Cell viability was not affected for hMSC-iCasp9 cells that were not treated with CID or hMSCs that did not possess iCasp9, as approximately 100% cell viability was observed in these control groups (Fig. 1A). The difference in cellular viability between treatment groups with CID and

those without CID was statistically significant ($P = 0.05$). The data suggest that CID has a cytotoxic effect on the hMSC-iCasp9 cells.

To confirm that the hMSC-iCasp9 cells could be used as a mechanism for regulated delivery of BMP2, the cells were transduced with AdBMP2. These cells were then subjected to either CID or vehicle for 48 h. Culture supernatant from the cells was collected daily, and BMP2 activity was measured on the BMP2-responsive cell line W20-17. These cells respond to BMP2 in the culture supernatant by expressing alkaline phosphatase (ALP) that can be measured and quantified [Olmsted et al., 2001]. The results suggest that BMP2 activity was present in all culture supernatant of the hMSCs-iCasp9 cells that received vehicle 48 h after transduction of the cells (Fig. 1B). Alternatively, culture supernatant from hMSCs-iCasp9 cells exposed to CID did not possess BMP2 activity and was not statistically different from the control (Fig. 1B). The negative control shows some alkaline phosphatase control cells; however, comparison of the results obtained from this control with supernatant from hMSCs-iCasp cells exposed to CID showed a significant change in levels of BMP2 activity (Fig. 1B).

The difference in ALP was statistically significant between groups treated with the CID compared to groups not treated with the CID. The ALP of the cells treated with the CID was similar to cell culture media alone (control) (Fig. 1B). The data suggest that the CID was able to stop the release of BMP2 from hMSC-iCasp9-AdBMP2 cells treated with 50 μg of CID.

The hMSC-iCasp9 cells were next encapsulated in the PEGDA hydrogel to confirm that the CID could freely diffuse into the microspheres to activate caspase 9 and apoptosis (Fig. 1C). The results suggest that the CID is able to enter the microspheres and induce cell death in the encapsulated cells as detected by the LIVE/DEAD assay. Further, quantification by counting and scoring cells in three independent fields revealed 75% of the cells were dead in the group treated with CID, whereas the vehicle treated was less than 1 percent dead. Although delivery of the CID to the microbeads appeared to reduce its efficacy slightly as compared to when it was delivered directly to the cells (Fig. 1A and C), the results showed significant cell death.

TERMINATION OF iRFP AND BMP2 EXPRESSION IN VIVO

To determine if delivery of the CID to mice could kill the cells encapsulated in the hydrogel, non-encapsulated and PEG-Da encapsulated AdBMP2-iRFP transduced hMSC-iCasp9 cells were injected into the hamstrings of NOD/SCID mice in the left and right leg, respectively. Mice also received an injection of either CID or vehicle. Far-red imaging for detection of iRFP fluorescence and quantification was done at daily intervals for 3 days; fluorescence intensities of both the directly injected and encapsulated cells appear to increase over the time period in mice receiving the vehicle (Fig. 2). As expected, significantly lower far-red fluorescence was observed in treatment groups injected with CID (Fig. 2). Surprisingly, there was a difference in fluorescence intensity between the directly injected AdBMP2 transduced cells and those that were encapsulated, which could be attributed to the physical barrier of the PEG-Da to the fluorescence (Fig. 2C). The data collectively suggests that delivery of CID resulted in a significantly lower level of far-red fluorescence, suggesting that

CID can block the production of iRFP and presumably BMP2 by most likely causing the cells that are encapsulated in hydrogel or directly injected to undergo apoptosis.

To confirm that BMP2 secretion was similarly affected by treatment with CID, bone formation was assessed at 10 days (Fig. 3). The results show that the animals that received CID did not form bone that was detectable either by microCT (Fig. 3A and B) or histology (Fig. 3C and D), whereas the groups receiving vehicle formed detectable bone. The resultant bone formation appeared to be dependent on the presence of CID but independent of whether the cells were encapsulated in the PEG-Da hydrogel, confirming that the CID could freely diffuse into the hydrogel microspheres to induce apoptosis. The data confirm that termination of the cells through activation of iCasp9 led to ablation of the BMP2 induced bone formation.

ADMINISTRATION OF CID STOPS BONE FORMATION PRIOR TO FORMATION OF MATRIX

Since the CID was delivered at the same time as BMP2 or at the induction of bone formation in the previous experiments, the timing of delivery of the CID was next varied to determine the effects of BMP2 withdrawal on bone formation at various times. In these experiments non-encapsulated and PEGDA-encapsulated hSC-iCasp9-AdBMP2-iRFP cells were injected into the hamstrings of NOD/SCID mice. CID was then administered 2, 4, 6, or 8 days after the initial induction of bone formation. The iRFP fluorescence was measured on days 1, 2, 5, 6, and 8 as a measure of BMP2 expression (Fig. 4A). In all groups, the iRFP expression was almost completely diminished 24 h after CID was administered (Fig. 4B), confirming that the iCasp9 safety switch was functioning as predicted in vivo.

Bone formation was then measured in all of the mice at 10 days to determine the effects of early termination of the BMP2 transduced cells. The results of microCT analysis showed the lack of bone formation in the group receiving CID on day 2 and a significant decrease in the group receiving the CID on day 4 (Fig. 4C and D). However, bone formation appeared to have progressed normally in those animals receiving CID on day 6 and 8, suggesting that removal of the cells at this stage of bone formation did not suppress the process (Fig. 4B and C). In all cases, bone formation appeared to progress normally in the vehicle treated groups.

DISCUSSION

Previous studies have demonstrated the ability of hydrogel-encapsulated cells transduced with AdBMP2 to form bone rapidly [Olabisi et al., 2010; Hsu et al., 2011]. In other studies, encapsulation of the cells in PEG-Da microspheres have led to avoidance of immune surveillance and clearance [Cruise et al., 1999]. Upon degradation, the PEG-Da microspheres can potentially release adenovirus from the delivery cells into the animals, resulting in transduction of host cells and potential secretion of BMP2 in tissues and possibly the circulation. In this way, unwanted bone formation could occur. Additionally, the transduced cells could lead to an undesirable immune response [Rezvani and Storb, 2012]. Further, given the current concerns of adverse events associated with recombinant BMP2 [Salisbury et al., 2011], providing surgeons a means to safely know they have terminated expression of the protein is a significant advantage. Therefore, these studies were designed

to determine if the clinically tested inducible caspase 9 system can effectively kill the AdBMP2 transduced cells within the hydrogel in order to terminate bone formation.

Although the cells, once killed, would presumably immediately stop secreting BMP2, in vitro experiments were designed to test this notion. The results demonstrated an almost immediate attenuation of BMP2 activity in the culture supernatant confirming other reports in the literature that suggest the protein in the absence of a carrier has a very short half-life. Next, experiments were performed to confirm that the CID could freely diffuse into the hydrogel microspheres and activate apoptosis in the adenovirus-transduced cells. In these experiments, apoptosis was not confirmed to be the mechanism of cellular death directly, due to technical limitations with immunostaining the cells within the beads. However, the mechanism of CID dimerization of the iCasp9 has been well documented in the literature. In these experiments, cell viability was used to determine the cellular response in the microspheres. The results confirmed that the small molecule could function similarly in the cells encapsulated in hydrogel as in those that were not encapsulated.

In order to follow these cells within the hydrogel microspheres, a far-red infrared imaging system was employed that was based on the iRFP promoter. Since the iCasp9 was previously incorporated into the hMSCs, the experiments could not be performed in an immune competent mouse; therefore, NOD/SCID mice were selected for all in vivo experiments. As expected, the directly injected cells could readily be observed in the animal, and the high sensitivity allowed the kinetics of transgene expression to be readily visualized. Surprisingly, the results of the far-red imaging revealed that steady-state levels of the iRFP transgene expression were not achieved until 72 h later. This finding was independent of whether the cells were encapsulated or directly injected. Such an increase in signal intensity over time was something that was not observed using either dsRED or luciferase imaging.

The far-red imaging allowed us to readily confirm the rapid termination of transgene in cells treated with CID. This was true regardless of whether cells were directly injected or encapsulated. Surprisingly, comparison of the signal in cells encapsulated in hydrogel to those directly injected showed a significant decrease. However, the sensitivity of the far-red imaging allowed for quantification of the signal in these animals and confirmed a significant difference between the group treated with vehicle and the one receiving CID.

To determine whether the safety switch could be effectively used to stop bone formation, experiments were designed to demonstrate this in vivo in mice. The results showed the complete ablation of bone formation in the group receiving CID, whereas bone formation progressed normally in the control group. These results appeared to be independent of encapsulation, supporting the idea that the attenuated iRFP signal was due to shielding of iRFP signal by the polymer rather than poor expression of the transgene. Since the microCT only detects mineralized bone, the samples that appeared negative by microCT were also analyzed histologically and confirmed to lack bone. Previous studies [Olmsted-Davis et al., 2002] with this model, demonstrated that bone formation progresses in a reproducible series of events, with the first appearance of bone matrix as early as 6–7 days after induction. Therefore, the lack of any stages of the bone formation in the tissues obtained from the

group that received the CID simultaneous with the AdBMP2-transduced cells suggests that bone formation did not progress in these animals.

CID was delivered at the start of bone formation to determine if the CID could successfully kill the cells and thus terminate the BMP2 expression. In subsequent experiments the timing of CID delivery was then varied to determine at what stage during the process the cells could be terminated and still result in bone. Surprisingly, termination of the cells, even as late as day 4, resulted in a significant reduction in bone formation. Previous experiments using this assay revealed a significant drop in the number of delivery cells approximately 5–6 days, regardless of whether the animal had a complete immune system [Olmsted-Davis et al., 2003]. Previous studies [Lazard et al., 2015] have shown this time correlates with the first appearance of osteoprogenitors and early cartilage. The small amount of bone formation may show that a small number of osteoprogenitors are within the tissue that are committed to becoming functional osteoblasts. The results suggest that even after recruitment of cells to the site of new bone, early removal of the BMP2 resulted in normal muscle tissues several days later. The cellular reaction present in the tissue was totally extinguished upon BMP2 withdrawal and did not result in formation of scar tissue.

Alternatively, it is not surprising that there appeared to be no effect on bone formation when the CID was given at 6 and 8 days after induction of bone formation, since the directly injected cells are generally cleared by this time. Histological analysis of the bone suggests that the process was similar to the group that received vehicle, and there was no detrimental effect on the newly forming bone.

Results of this study show the requirement for BMP2 to be present until the early osteoblasts are present at the site of the newly forming bone and early termination of BMP2 expression prior to this stage results in the suspension of bone formation. This finding is important to the field of bone tissue engineering where recombinant protein is being delivered using a variety of scaffolds [King and Krebsbach, 2012; Waldorff et al., 2013; Patel et al., 2015]. The data suggest that the protein must be present throughout the bone formation process, emphasizing the need for methods that will allow the protein to be stable and available for longer periods of time. Additionally, this study is the first to provide detailed information about the mechanism of BMP2-induced bone formation and provides additional caveats about stopping BMP2-induced bone formation. Alternatively, considering the short half-life of the BMP2 protein, the findings support the idea of cellular delivery of the protein at the target site, which can continually replenish the protein source. Further, the findings also support that cell-based gene therapy approaches for targeted bone repair can be safely implemented by providing a mechanism to rapidly remove the adenovirus-transduced cells without destruction of the newly forming bone.

Acknowledgments

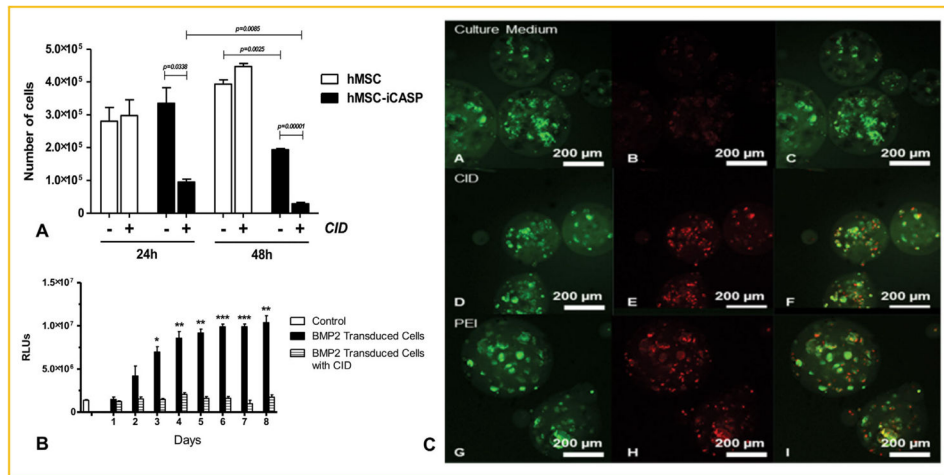
Grant sponsor: U.S. Department of Defense; Grant numbers: DAMD07128004, PR110222, PR110623.

This work was supported by the Department of Defense grants DAMD07128004, DOD PR110222, and DOD PR110623. Additionally, we would like to thank Dr. Carlos Ramos, MD, for the gift of the hMSCs and hMCs-iCasp9. We would also like to thank Rete Nistal for her assistance in generating all the tissues sections required for histological analysis.

References

- Acton, QA. ScholarlyEditions. 2012. Bone morphogenetic proteins: Advances in research and application: 2011 Edition: ScholarlyBrief.
- Azhdarinia A, Wilganowski N, Robinson H, Ghosh P, Kwon S, Lazard ZW, Davis AR, Olmsted-Davis E, Sevick-Muraca EM. Characterization of chemical, radiochemical and optical properties of a dual-labeled MMP-9 targeting peptide. *Bioorg Med Chem*. 2011; 19:3769–3776. [PubMed: 21612930]
- Boerckel JD, Kolambkar YM, Dupont KM, Uhrig BA, Phelps EA, Stevens HY, Garcia AJ, Guldberg RE. Effects of protein dose and delivery system on BMP-mediated bone regeneration. *Biomaterials*. 2011; 32:5241–5251. [PubMed: 21507479]
- Carragee EJ, Hurwitz EL, Weiner BK. A critical review of recombinant human bone morphogenetic protein-2 trials in spinal surgery: Emerging safety concerns and lessons learned. *Spine J*. 2011; 11:471–491. [PubMed: 21729796]
- Cruise GM, Hegre OD, Lamberti FV, Hager SR, Hill R, Scharp DS, Hubbell JA. In vitro and in vivo performance of porcine islets encapsulated in interfacially photopolymerized poly(ethylene glycol) diacrylate membranes. *Cell Transplant*. 1999; 8:293–306. [PubMed: 10442742]
- Di Stasi A, Tey SK, Dotti G, Fujita Y, Kennedy-Nasser A, Martinez C, Straathof K, Liu E, Durett AG, Grilley B, Liu H, Cruz CR, Savoldo B, Gee AP, Schindler J, Krance RA, Heslop HE, Spencer DM, Rooney CM, Brenner MK. Inducible apoptosis as a safety switch for adoptive cell therapy. *N Engl J Med*. 2011; 365:1673–1683. [PubMed: 22047558]
- Dmitriev AE, Farhang S, Lehman RA Jr, Ling GS, Symes AJ. Bone morphogenetic protein-2 used in spinal fusion with spinal cord injury penetrates intrathecally and elicits a functional signaling cascade. *Spine J*. 2010; 10:16–25. [PubMed: 19914878]
- Dmitriev AE, Lehman RA Jr, Symes AJ. Bone morphogenetic protein-2 and spinal arthrodesis: The basic science perspective on protein interaction with the nervous system. *Spine J*. 2011; 11:500–505. [PubMed: 21729799]
- Engstrand T, Daluiski A, Bahamonde ME, Melhus H, Lyons KM. Transient production of bone morphogenetic protein 2 by allogeneic transplanted transduced cells induces bone formation. *Hum Gene Ther*. 2000; 11:205–211. [PubMed: 10646651]
- Fouletier-Dilling CM, Bosch P, Davis AR, Shafer JA, Stice SL, Gugala Z, Gannon FH, Olmsted-Davis EA. Novel compound enables high-level adenovirus transduction in the absence of an adenovirus-specific receptor. *Hum Gene Ther*. 2005; 16:1287–1297. [PubMed: 16259562]
- Govender S, Csimma C, Genant HK, Valentin-Opran A, Amit Y, Arbel R, Aro H, Atar D, Bishay M, Borner MG, Chiron P, Choong P, Cinats J, Courtenay B, Feibel R, Geulette B, Gravel C, Haas N, Raschke M, Hammacher E, van der Velde D, Hardy P, Holt M, Josten C, Ketterl RL, Lindeque B, Lob G, Mathevon H, McCoy G, Marsh D, Miller R, Munting E, Oevre S, Nordsletten L, Patel A, Pohl A, Rennie W, Reynders P, Rommens PM, Rondia J, Rossouw WC, Daneel PJ, Ruff S, Ruter A, Santavirta S, Schildhauer TA, Gekle C, Schnettler R, Segal D, Seiler H, Snowdowne RB, Stapert J, Taglang G, Verdonk R, Vogels L, Weckbach A, Wentzensen A, Wisniewski T. Group BMPEiSfTTS. Recombinant human bone morphogenetic protein-2 for treatment of open tibial fractures: A prospective, controlled, randomized study of four hundred and fifty patients. *J Bone Joint Surg Am*. 2002; 84-A:2123–2134. [PubMed: 12473698]
- Gugala Z, Davis AR, Fouletier-Dilling CM, Gannon FH, Lindsey RW, Olmsted-Davis EA. Adenovirus BMP2-induced osteogenesis in combination with collagen carriers. *Biomaterials*. 2007; 28:4469–4479. [PubMed: 17645942]
- Hsu CW, Olabisi RM, Olmsted-Davis EA, Davis AR, West JL. Cathepsin K-sensitive poly(ethylene glycol) hydrogels for degradation in response to bone resorption. *J Biomed Mater Res A*. 2011; 98:53–62. [PubMed: 21523904]
- Huang H, Wismeijer D, Hunziker EB, Wu G. The acute inflammatory response to absorbed collagen sponge is not enhanced by BMP-2. *Int J Mol Sci*. 2017; 18:1–11.
- King WJ, Krebsbach PH. Growth factor delivery: How surface interactions modulate release in vitro and in vivo. *Adv Drug Deliv Rev*. 2012; 64:1239–1256. [PubMed: 22433783]

- Lazard ZW, Olmsted-Davis EA, Salisbury EA, Gugala Z, Sonnet C, Davis EL, Beal E 2nd, Ubogu EE, Davis AR. Osteoblasts have a neural origin in heterotopic ossification. *Clin Orthop Relat Res*. 2015; 473:2790–2806. [PubMed: 25944403]
- Levy RJ, Schoen FJ, Sherman FS, Nichols J, Hawley MA, Lund SA. Calcification of subcutaneously implanted type I collagen sponges. Effects of formaldehyde and glutaraldehyde pretreatments. *Am J Pathol*. 1986; 122:71–82. [PubMed: 3079959]
- Lo KW, Ulery BD, Ashe KM, Laurencin CT. Studies of bone morphogenetic protein-based surgical repair. *Adv Drug Deliv Rev*. 2012; 64:1277–1291. [PubMed: 22512928]
- Olabisi RM, Lazard ZW, Franco CL, Hall MA, Kwon SK, Sevick-Muraca EM, Hipp JA, Davis AR, Olmsted-Davis EA, West JL. Hydrogel microsphere encapsulation of a cell-based gene therapy system increases cell survival of injected cells, transgene expression, and bone volume in a model of heterotopic ossification. *Tissue Eng Part A*. 2010; 16:3727–3736. [PubMed: 20673027]
- Olmsted EA, Blum JS, Rill D, Yotnda P, Gugala Z, Lindsey RW, Davis AR. Adenovirus-mediated BMP2 expression in human bone marrow stromal cells. *J Cell Biochem*. 2001; 82:11–21. [PubMed: 11400159]
- Olmsted-Davis EA, Gugala Z, Camargo F, Gannon FH, Jackson K, Kienstra KA, Shine HD, Lindsey RW, Hirschi KK, Goodell MA, Brenner MK, Davis AR. Primitive adult hematopoietic stem cells can function as osteoblast precursors. *Proc Natl Acad Sci USA*. 2003; 100:15877–15882. [PubMed: 14673088]
- Olmsted-Davis EA, Gugala Z, Gannon FH, Yotnda P, McAlhany RE, Lindsey RW, Davis AR. Use of a chimeric adenovirus vector enhances BMP2 production and bone formation. *Hum Gene Ther*. 2002; 13:1337–1347. [PubMed: 12162816]
- Partridge KA, Oreffo RO. Gene delivery in bone tissue engineering: Progress and prospects using viral and nonviral strategies. *Tissue Eng*. 2004; 10:295–307. [PubMed: 15009954]
- Patel JJ, Flanagan CL, Hollister SJ. Bone morphogenetic protein-2 adsorption onto poly- ϵ -caprolactone better preserves bioactivity in vitro and produces more bone in vivo than conjugation under clinically relevant loading scenarios. *Tissue Eng Part C Methods*. 2015; 21:489–498. [PubMed: 25345571]
- Rezvani AR, Storb RF. Prevention of graft-vs.-host disease. *Expert Opin Pharmacother*. 2012; 13:1737–1750. [PubMed: 22770714]
- Sadelain M. Insertional oncogenesis in gene therapy: How much of a risk? *Gene Ther*. 2004; 11:569–573. [PubMed: 15029226]
- Salisbury EA, Olmsted-Davis EA, Davis AR. Adverse events and bone morphogenetic protein-2. *Spine J*. 2011; 11:802. [PubMed: 21925422]
- Stiehler M, Duch M, Mygind T, Li H, Ulrich-Vinther M, Modin C, Baatrup A, Lind M, Pedersen FS, Bunger CE. Optimizing viral and non-viral gene transfer methods for genetic modification of porcine mesenchymal stem cells. *Adv Exp Med Biol*. 2006; 585:31–48. [PubMed: 17120775]
- Straathof KC, Pule MA, Yotnda P, Dotti G, Vanin EF, Brenner MK, Heslop HE, Spencer DM, Rooney CM. An inducible caspase 9 safety switch for T-cell therapy. *Blood*. 2005; 105:4247–4254. [PubMed: 15728125]
- VandenDriessche T, Chuah MK. Hitting the target without pulling the trigger. *Mol Ther*. 2015; 23:4–6. [PubMed: 25561034]
- Waldorff EI, Roessler BJ, Zachos TA, Miller BS, McHugh J, Goldstein SA. Preclinical evaluation of a novel implant for treatment of a full-thickness distal femoral focal cartilage defect. *J Arthroplasty*. 2013; 28:1421–1429. [PubMed: 23523501]
- Zhou X, Dotti G, Krance RA, Martinez CA, Naik S, Kamble RT, Durett AG, Dakhova O, Savoldo B, Di Stasi A, Spencer DM, Lin YF, Liu H, Grilley BJ, Gee AP, Rooney CM, Heslop HE, Brenner MK. Inducible caspase-9 suicide gene controls adverse effects from alloplete T cells after haploidentical stem cell transplantation. *Blood*. 2015; 125:4103–4113. [PubMed: 25977584]

**Fig. 1.**

(A) Cell viability of human mesenchymal stem cells possessing a stably integrated inducible caspase 9 (iCasp9) when treated with a chemical inducer of dimerization (CID) or vehicle. All data are reported as the mean \pm standard deviation for $n = 3$. (B) Quantification of alkaline phosphatase (ALP) in W20-17 cells. Media collected from the AdBMP2-transduced hMSCs-iCasp9 cells cultured in the presence of CID or vehicle was added to culture media of W20-17 cells, and 72 h later alkaline phosphatase activity was measured by a chemiluminescent assay. Alkaline phosphatase activity was reported in relative luminescence units (RLUs). All data are reported as the mean \pm standard error of the mean for $n = 3$. * Represents significant difference between groups ($P < 0.05$). (C) LIVE/DEAD staining cultured in complete medium after 24 h. Cells in culture medium (A–C), in the presence of 50 μg of a chemical inducer of dimerization (CID) and 100 ng/ml polyethylenimine (PEI). Maximum intensity projection of green (FITC) channel (A,D,G), red (rhodamine) channel (B,E,H), and merge of all channels (C,F,I). Dead cells appear red and live cells appear green; 20 \times mag.

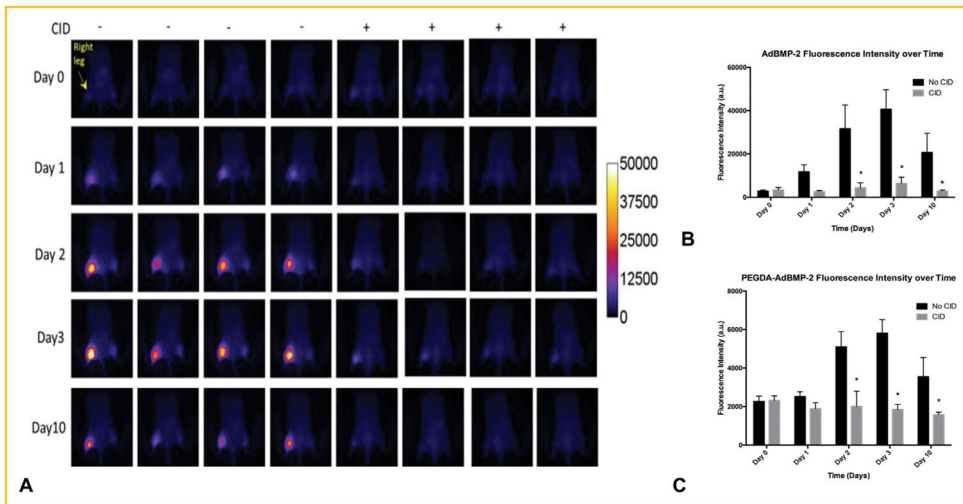


Fig. 2. (A) Far-red fluorescence emission after (B) direct injection or (C) encapsulation in PEGDA hydrogel of AdBMP2-AdiRFP transduced hMSC-iCasp9 cells into NOD/SCID mice in the presence or absence of CID. Quantification of fluorescence intensity in mice receiving these cells (Day 0) in the absence and presence of CID was reported as the mean \pm standard error of the mean for $n = 4$. * Represents significant difference of fluorescence intensity between groups ($P < 0.05$).

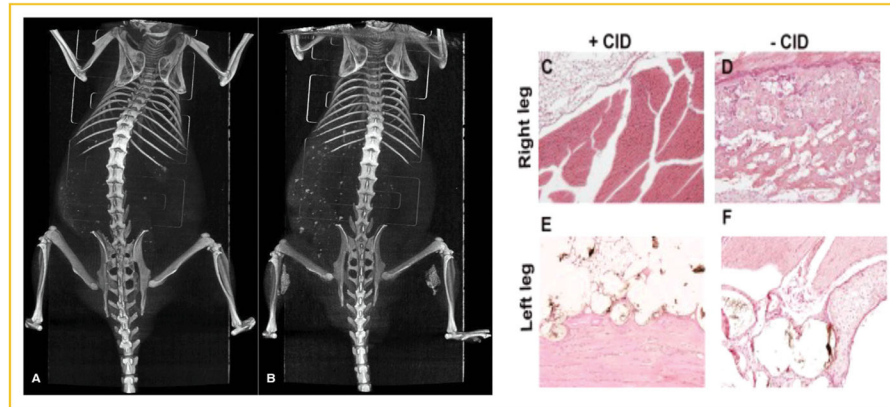


Fig. 3. MicroCT analysis of tissues 2 weeks after intramuscular delivery of AdBMP2-transduced hMSCs possessing the inducible caspase 9 (iCasp9). (A) Representative three-dimensional reconstruction of bone formation in mice treated with chemical inducer of dimerization (CID, 50 μ g) compared to (B) mice treated with vehicle. (C–F) Representative photomicrographs of hematoxylin and eosin stained section of the newly forming bone.

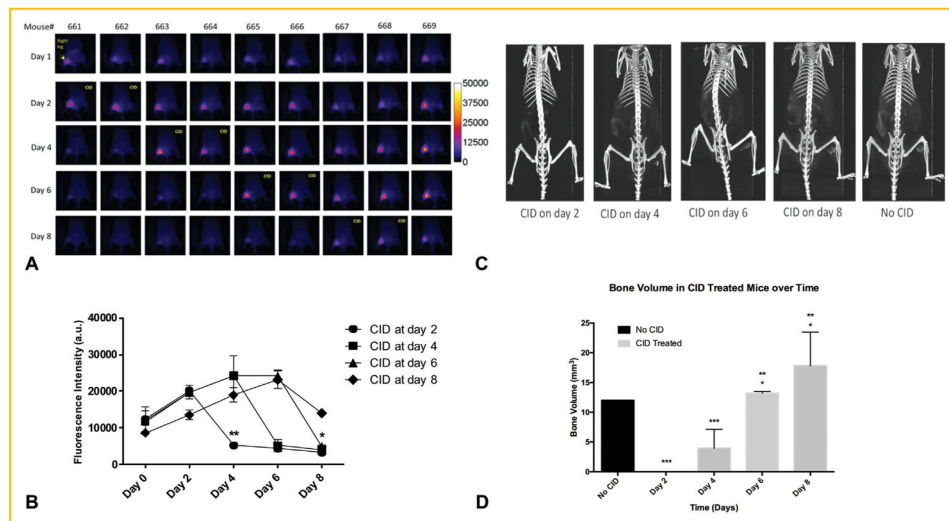


Fig. 4. Mice exposed to CID or vehicle at 2, 4, 6, and 8 days after injection of AdBMP2-AdiRFP transduced hMSCs-iCasp9 cells during the formation of heterotopic bone formation. (A) Far-red fluorescence expression in the mice. (B) Quantification of far-red fluorescence in the mice. (C) Representative three-dimensional reconstructions of the microCT data collected from imaging the mice. (D) Quantification of bone volume in the mice. All data are reported as the mean \pm standard error of the mean for $n = 3$. * Represents significant difference between groups ($P < 0.05$).